BRAIN CONNECTIVITY
Volume 12, Number 1, 2022
Mary Ann Liebert, Inc.
DOI: 10.1089/brain.2021.0047

REVIEW ARTICLE

Microstructure-Weighted Connectomics in Multiple Sclerosis

Sara Bosticardo,[1,*] Simona Schiavi,[1,*] Sabine Schaedelin,[2] Po-Jui Lu,[3,4] Muhamed Barakovic,[3,4] Matthias Weigel,[3–5] Ludwig Kappos,[3,4] Jens Kuhle,[2–4] Alessandro Daducci,[1,†] and Cristina Granziera[2–4,†]

Abstract

Introduction: Graph theory has been applied to study the pathophysiology of multiple sclerosis (MS) since it provides global and focal measures of brain network properties that are affected by MS. Typically, the connection strength and, consequently, the network properties are computed by counting the number of streamlines (NOS) connecting couples of gray matter regions. However, recent studies have shown that this method is not quantitative.
Methods: We evaluated diffusion-based microstructural measures extracted from three different models to assess the network properties in a group of 66 MS patients and 64 healthy subjects. Besides, we assessed their correlation with patients' disability and with a biological measure of neuroaxonal damage.
Results: Graph metrics extracted from connectomes weighted by intra-axonal microstructural components were the most sensitive to MS pathology and the most related to clinical disability. In contrast, measures of network segregation extracted from the connectomes weighted by maps describing extracellular diffusivity were the most related to serum concentration of neurofilament light chain. Network properties assessed with NOS were neither sensitive to MS pathology nor correlated with clinical and pathological measures of disease impact in MS patients.
Conclusion: Using tractometry-derived graph measures in MS patients, we identified a set of metrics based on microstructural components that are highly sensitive to the disease and that provide sensitive correlates of clinical and biological deterioration in MS patients.

Keywords: diffusion microstructure; graph theory; multiple sclerosis; structural connectivity; tractography; tractometry

Impact Statement

Graph theory has been widely used to study the alterations in the structural connectivity of multiple sclerosis (MS) patients. Usually, brain graphs used for the extraction of network metrics are created by counting the number of streamlines connecting gray matter regions, however, this method is not quantitative. In this study, we used tractometry to average the values of diffusion-based microstructural maps along the reconstructed streamlines. Our results show that network metrics extracted from the connectomes weighted on microstructural maps provide sensitive information to MS pathology, which correlate with clinical and biological measures of disease impact.

[1]Diffusion Imaging and Connectivity Estimation (DICE) Lab, Department of Computer Science, University of Verona, Verona, Italy.
[2]Neurology Clinic and Policlinic, Departments of Medicine, Clinical Research and Biomedical Engineering, University Hospital Basel and University of Basel, Basel, Switzerland.
[3]Translational Imaging in Neurology (ThINk), Department of Biomedical Engineering, University Hospital Basel and University of Basel, Basel, Switzerland.
[4]Research Center for Clinical Neuroimmunology and Neuroscience (RC2NB) Basel, University Hospital Basel and University of Basel, Basel, Switzerland.
[5]Division of Radiological Physics, Department of Radiology, University Hospital Basel, Basel, Switzerland.
*Equally contributed (share first authorship).
†Equally contributed (share last authorship).

© Sara Bosticardo *et al.* 2021; Published by Mary Ann Liebert, Inc. This Open Access article is distributed under the terms of the Creative Commons Attribution Noncommercial License [CC-BY-NC] (http://creativecommons.org/licenses/by-nc/4.0/) which permits any noncommercial use, distribution, and reproduction in any medium, provided the original author(s) and the source are cited.

Introduction

Multiple sclerosis (MS) is a disease of the nervous systems characterized by focal and diffuse inflammation and degeneration, which variably affect structural and functional connectivity (Rolak, 2003). Demyelination and axonal degeneration are cardinal features of MS, which affect specific tracts but also alter brain networks, both locally and globally (Rolak, 2003).

Hence, methods to assess global and local network properties are valuable to investigate the pathophysiology of MS, as well as to better understand its clinical and biological impact.

Tractography allows reconstructing noninvasively the major fiber tracts of the white matter (WM), which are identified through ''streamlines'' (Yeh et al., 2020). The map of streamlines—that is, structural connections of the brain that form a ''connectome''—can be modeled as a network, where nodes correspond to gray matter regions and edges represent the streamline connections between pairs of them (Sotiropoulos and Zalesky, 2019).

The weight of an edge in a connectome reflects the interregional connection strength between brain regions and aims to characterize biologically interpretable properties such as axon density and demyelination (Kamagata et al., 2019). This network formalism (graph theory) allows characterizing brain connectivity *in vivo* and studying a wide range of neurological diseases (Sotiropoulos and Zalesky, 2019). Graph theory permits in fact the analysis of connectivity at the topological level by extracting some metrics that may capture pathology-related alterations (Van Wijk et al., 2010).

The most common strategy to weight connectome edges is based on counting the number of streamlines (NOS) connecting each pair of regions (Jones et al., 2013; Sotiropoulos and Zalesky, 2019). However, recent studies have highlighted that this approach lacks specificity and it is not quantitative in fact, tractography algorithms, propagate through the estimated fiber orientation without considering the density of the underlying bundles. Thus, although tractography is very effective in recovering the major fiber pathways, it does not inform about the number of axons constituting these fiber bundles (axon density). For this reason, NOS cannot be considered a valid biomarker of the strength of connection between regions (Jones et al., 2013; Sotiropoulos and Zalesky, 2019; Yeh et al., 2020).

To retrieve information on the underlying tissue and, in turn, to get more biologically interpretable properties, several microstructural diffusion-based models have been combined with the estimated streamlines (Bells et al., 2011).

The most common model is diffusion tensor imaging (DTI) that characterizes the measured diffusion displacement as a three-dimensional (3D) Gaussian process, which completely describes the molecular mobility along each axis and the correlation between the movements and the axes (Descoteaux, 2008; Le Bihan et al., 2001). However, DTI assumes a single fiber population in each voxel, therefore, it does not provide sufficient information of the individual tissue microstructure features. However, more advanced models have the ability to isolate the signal contribution from different tissue compartments, further increasing the specificity to different tissue subtypes (Alexander et al., 2019). These models include neurite orientation dispersion and density imaging (NODDI) (Zhang et al., 2012) and spherical mean technique (SMT) (Kaden et al., 2015, 2016).

NODDI explicitly takes orientation dispersion of the neurites into account and models three microstructural environments in a voxel: *intracellular* (or intra-axonal), *extracellular* (or extra-axonal), and *cerebral spinal fluid* (or free water) compartments (Zhang et al., 2012). SMT, instead, investigates the tissue microscopic features independently from the fiber's orientation. This characteristic allows minimizing the confounding effects derived from fiber crossing, curving, and orientation dispersion. Furthermore, this method exploits a microscopic diffusion model that describes the signal coming from the tissue microenvironment to estimate the microscopic features specific to the *intraneurite* and *extraneurite* compartments (Kaden et al., 2015, 2016).

The analysis of the connectomes with graph theory has been previously applied to MS patients (Fleischer et al., 2019; Kocevar et al., 2016; Li et al., 2013; Nigro et al., 2015; Ozturk et al., 2010; Pagani et al., 2020; Pardini et al., 2015; Rocca et al., 2016; Schiavi et al., 2020b). The results of studies comparing MS patients with healthy controls (HCs) have shown that different global structural network changes occur in MS patients (Fleischer et al., 2019; Kocevar et al., 2016; Li et al., 2013; Nigro et al., 2015; Ozturk et al., 2010; Pagani et al., 2020; Pardini et al., 2015; Rocca et al., 2016; Schiavi et al., 2020b). Some studies evidenced that transferring and processing of information within the networks of patients with MS are less efficient with respect to HCs (He et al., 2009; Schiavi et al., 2020b; Shu et al., 2011), whereas other studies revealed an increase in network segregation in MS patients compared with HCs (Gamboa et al., 2014; Llufriu et al., 2017; Richiardi et al., 2012; Rocca et al., 2010; Schiavi et al., 2020b; Tewarie et al., 2014).

In this study, we investigated the pathology-related alterations in connectomes of MS patients compared with HCs using *tractometry* (Bells et al., 2011). This technique weights the connections obtained from tractography by averaging the tissue properties estimated from diffusion-based microstructural maps along their paths, hereby providing more quantitative estimates than the NOS and better biological interpretability. More precisely, we investigated which microstructural maps and which global network metrics extracted from them are more sensitive to alterations in the structural connectivity of MS patients. Furthermore, we performed a clinical and biological validation of tractometry by assessing their relationship with (1) the *Expanded Disability Status Scale* (EDSS) (Kurtzke, 2009) and (2) serum neurofilament light polypeptide (sNfL) levels, which is a promising biomarker of neuroaxonal injury (Khalil et al., 2018).

Subjects/Materials and Methods

Subjects

Sixty-six MS patients (39 females, 43.9 ± 14.5 years, 20 primary/secondary progressive, and 46 relapsing remitting) and sixty-four HCs (38 females, 36.9 ± 12.8 years) were enrolled in this study, refer to Table 1 for more details. The inclusion criteria for the enrollment of MS patients included (1) age between 18 and 75 years, (2) MS diagnosis fulfilling McDonald criteria (Thompson et al., 2018), (3) absence of neurological or psychiatric disease other than MS, and (4) absence of contraindications in subjects for magnetic resonance imaging (MRI). MRI and sNfL were assessed at

Table 1. Demographic and Clinical Characteristic of Multiple Sclerosis Patients and Healthy Controls

Group	TOT	M	F	Age (years) mean ± SD	EDSS median (min–max)	NfL (pg/mL) mean (min–max)	T2 lesion volume (mm^3) mean ± SD
HC	64	26	38	36.9 ± 12.8	/	/	/
RR	46	16	30	37.3 ± 11.7	1.5 (0–4)	7.4 (2.4–13.9)	6017.0 ± 7123.0
PP	10	7	3	58.0 ± 8.3	4 (2–6)	11.0 (4.7–17.1)	15,719.0 ± 13,402.0
SP	10	4	6	60.2 ± 5.5	6.1 (3.5–8)	14.3 (7.9–23.8)	16,431.0 ± 18,679.0

Demographic and clinical characteristics of MS patients (divided according to the clinical phenotype of the disease) and HCs.
EDSS, expanded disability status scale; F, female; HCs, healthy controls; M, male; max, maximum; min, minimum; MS, multiple sclerosis; NfL, neurofilament light polypeptide; PP, primary progressive MS patients; RR, relapsing remitting MS patients; SD, standard deviation; SP, secondary progressive MS patients; TOT, total.

least 3 months after a clinical relapse/corticosteroid treatment and the assessment of disability scores (EDSS) was performed within 3 months from the MRI in case of clinically stable patients (Disanto et al., 2017).

The ethical review committee of the University Hospital Basel (IRB of Northwest Switzerland) approved the study, and all participants entered the study after written consent.

MRI acquisition

All subjects underwent MRI on a 3T system (Prisma; Siemens Healthcare, Erlangen, Germany) with 64-channel head and neck coil. The acquisition protocol included (1) 3D FLAIR (repetition time [TR]/echo time [TE]/inversion time [TI] = 5000/386/1800 ms) 1 mm^3 isotropic spatial resolution; (2) 3D MP2RAGE (TR/TI1/TI2 = 5000/700/2500 ms) 1 mm^3 isotropic spatial resolution; and (3) multishell diffusion (TR/TE/impulse duration [d]/time between impulses [D] = 4.5 s/75 ms/19 ms/36 ms) 1.8 mm^3 isotropic spatial resolution with b values 700/1000/2000/3000 s/mm^2 and 6/20/45/66 diffusion directions, respectively, per shell, and 12 measurements at b value 0 s/mm^2 with both anterior to posterior and *reversed phase encoding*.

Anatomical images

MS lesions were semiautomatically segmented with an automatic in-house deep learning-based method (La Rosa et al., 2020), followed by manual correction. This method takes as input both FLAIR and MP2RAGE MRI contrasts and consists of two convolutional neural networks. Thus, WM lesion masks were manually corrected on the FLAIR sequences and filled on the T1 images to improve the registration and the segmentation steps on the patients' images.

We processed T1-filled images with FreeSurfer and we used the standard Desikan–Killiany atlas (Desikan et al., 2006) for the automatic segmentation that provides cortical and subcortical parcellation of 85 (42 for hemisphere + brainstem) regions of interest.

Diffusion MRI processing

Diffusion MR images were corrected for movement artifacts and susceptibility induced distortions using *eddy* and *top-up* commands from FMRIB Software Library (FSL) (Gibbs and Liu, 2015; Horsfield, 1999; Yamada et al., 2014). To reconstruct the whole brain anatomically constrained tractography, we performed the five-tissue-type segmentation on T1 images using MRtrix3 (Tournier et al., 2019), a step that is necessary to retrieve the tissue information according to the FSL algorithm (Smith et al., 2012). Once the five tissues were obtained, they were registered to the diffusion space using FMRIB's linear image registration tool with boundary-based algorithm provided by FSL (Jenkinson et al., 2002). We estimated the response functions for each individual tissue type, as segmented by T1, to perform multitissue spherical deconvolution, and we generated 3 millions of streamlines using the iFOD2 algorithm of MRtrix3 (Tournier et al., 2019).

To reduce the incidence of false positives that are typical of probabilistic tractography (Sarwar et al., 2019), we set the power parameter to 3. The power option, in fact, directly influences the magnitude of the conservative estimates of fiber orientation used by iFOD2. With a power of infinity, theoretically, iFOD2 is turned into a deterministic algorithm that is known to find fewer false positives at the price of potentially introducing false negative. However, because of the loss of tissue and edema in the lesion areas, a pure deterministic algorithm might be less efficient in reconstructing all the pathways in MS patients. Thus, we tuned this parameter by visually inspecting the tractographies.

To compute microstructural maps from the DTI model, we used the measurements with $b \leq 1000$ s/mm^2 for the fitting of the diffusion tensor in FSL (O'Donnell and Westin, 2011). We retrieved the microstructural maps of fractional anisotropy (FA), mean diffusivity (MD), and radial diffusivity (RD). The first describes the degree of the diffusion process anisotropy, the second is the mean of the three eigenvalues of the diffusion tensor, whereas the third describes the diffusion perpendicular to the main diffusion direction (Le Bihan et al., 2001). To fit the NODDI model, we used the AMICO software (Daducci et al., 2015) on measurements with $b \leq 2000$ s/mm^2 and obtained the maps of intraneurite volume fraction (ICVF) and isotropic volume fraction (ISOVF). The former describes the intracellular environment, whereas the latter describes the free water in the extracellular environment (Zhang et al., 2012).

For the extraction of microstructural maps from SMT, we used the open-source code available at https://github.com/ekaden/smt, on measurements with $b \leq 2000$ s/mm^2 (Devan et al., 2020). We extracted the microstructural maps of neurite volume fraction (INTRA), extraneurite transverse diffusivity (EXTRATRANS), and extraneurite mean diffusivity (EXTRAMD) that describe the intracellular compartment, the anisotropic extraneurite compartment including its transverse microscopic diffusivity and the signal outside the axons, respectively (Kaden et al., 2015, 2016).

Connectome estimation

As reported in Figure 1, we generated the connectomes using the cortical and the subcortical regions of gray matter as nodes and the estimated streamlines as edges with different weights. For the NOS, we created a matrix containing in each cell the NOS that start from one region and arrive in another region (0 = no connection).

To obtain the other connectomes, we used *tractometry* and computed the average value along the tracts of the previously described scalar maps extracted from the microstructural models DTI, NODDI, and SMT to assess the connectivity in a more quantitative way. These maps, in fact, provide information on the morphological structure of axons. To achieve this, using MRtrix3 (Tournier et al., 2019), we sampled the streamlines of each bundle in n points and then we averaged the values of the microstructural maps described in Diffusion MRI Processing section evaluated at those spatial coordinates. This approach is expected to produce more quantitative estimates of the connectivity that are presumed to lead to a better interpretation of biological features (Bells et al., 2011).

Network metrics

As suggested in Sotiropoulos and Zalesky (2019), we filtered the connectomes by removing the connections that were not present in at least 50% of HCs, to remove eventual spurious WM connections (Buchanan et al., 2020; Zalesky et al., 2010).

To remove eventual bias coming from the ease in tracking shorter connections, we also zeroed all the values on the diagonal (Griffa et al., 2013). Then, we used Brain Connectivity Toolbox to extract from each connectome five global network metrics: density, which is the ratio between actual and possible connections, efficiency, which corresponds to the average inverse shortest weighted path length and is inversely related to the characteristic path length, modularity, which reflects the network segregation, clustering coefficient, which indicates the degree on which nodes tend to cluster together, and mean strength, which corresponds to all the nodal strength average where the nodal strength is defined as the sum of the edges' weight connected to a node.

The algorithms that are usually applied for the extraction of network metrics explicitly assume that in weighted brain networks, edges with the highest weights delineate the strongest and most reliable connections (Zalesky et al., 2010). However, in our study, we have also weighted the connections with MD, RD, ISOVF, EXTRATRANS, and EXTRAMD maps. According to this weighting approach, edges with high values may represent connections that traverse voxels characterized by the presence of cerebrospinal fluid. Thus, high edge weights do not indicate stronger connections and violate the underlying assumptions for network analysis. To avoid this issue, as suggested in Zalesky et al. (2010), we applied the negative logarithm transformation to each entry of these weighted connectomes, to consider the edges with the original lower weights as the most likely communication paths.

Statistical analysis

The statistical analysis was performed in R using robust models to account for eventual outliers (Koller and Stahel, 2011). First, we tested the differences in density among the two groups of subjects using a robust linear model with age

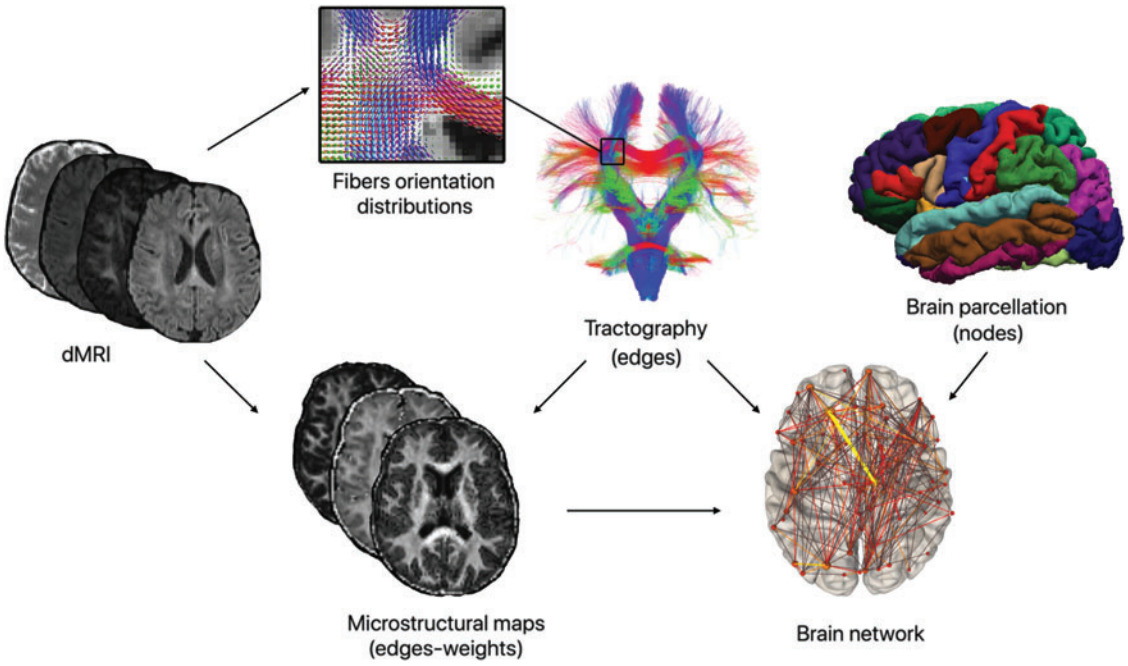

FIG. 1. Pipeline for the construction of brain graphs weighed using tractometry. By combining the parcellation of gray matter regions, the streamlines computed using tractography, and the different diffusion-based microstructural maps, we obtained the weighted connectomes. Using these weighted connectomes, we built the brain graphs from which we calculated the global network metrics to analyze the topological properties of the networks. dMRI, diffusion-weighted magnetic resonance images. Color images are available online.

and gender as covariate. Density was significantly different between HCs and MS patients ($p < 0.001$). We then tested the relationship between density and T2 lesion volumes using Pearson correlation, accounting for gender and age as covariates. As expected, Figure 2 shows that density is negatively related with the volume of the WM lesions ($p < 0.001$, $\sigma = -0.611$). Thus, in accordance with what is reported in Schiavi et al. (2020b) and Van Wijk et al. (2010), we added this variable among the confounding factors.

We tested the H_0-1 that there are no differences among network metrics when they are extracted from a connectome weighted for each of the nine considered microstructural measures; we also assessed the H_0-2 that there are no differences in network metrics between MS patients and HCs when each network metric is extracted from a connectome weighted for DTI, NODDI, and SMT.

We report p values adjusted for multiple comparisons with Holm test (Aickin and Gensler, 1996) for both H_0-1 (4 comparisons for each microstructural measure) and H_0-2 (12 comparisons for DTI, NODDI, and SMT, respectively). Finally, network metrics extracted from each connectome were evaluated (1) in a robust linear model adjusted for gender, age, and disease duration to evaluate their contributions in explaining the worsening of motor disability measured through the EDSS and (2) in a robust linear model adjusted for gender and age to evaluate whether the alterations of MS patient's structural connectivity are related to the sNfL increase.

Results

Results of groups comparison are reported in Table 2. The values that reached statistical significance are highlighted in bold, and the corresponding violin plots are shown in Figure 3.

Our results refute the first H_0 hypothesis showing that (1) when the network analysis was performed with tractometry derived from DTI-MD, DTI-RD, and SMT-EXTRATRANS, there was a significant decrease in global efficiency and in mean strength in MS patients compared with HCs, and that (2) if the network analysis was performed with tractometry derived from NODDI-ICVF and SMT-INTRA, there were both a significant decrease in global efficiency, clustering coefficient, and mean strength and a significant increase in modularity of MS patients compared with HCs.

Interestingly, when the network analysis was performed using NOS-weighted connectomes, there were no significant differences between patients and controls surviving the use of density as a confounding factor.

When we tested the second H_0 hypothesis, the network analysis using tractometry derived from NODDI-ICVF appeared to be the most sensitive. In fact, the mean strength extracted from ICVF showed statistically significant differences between MS and HCs, and other network metrics obtained using this map show similar results without reaching statistical significance.

Among the tested maps, we found that network metrics computed by weighting the connectomes with NODDI-ICVF and SMT-INTRA well explained the EDSS (adjusted

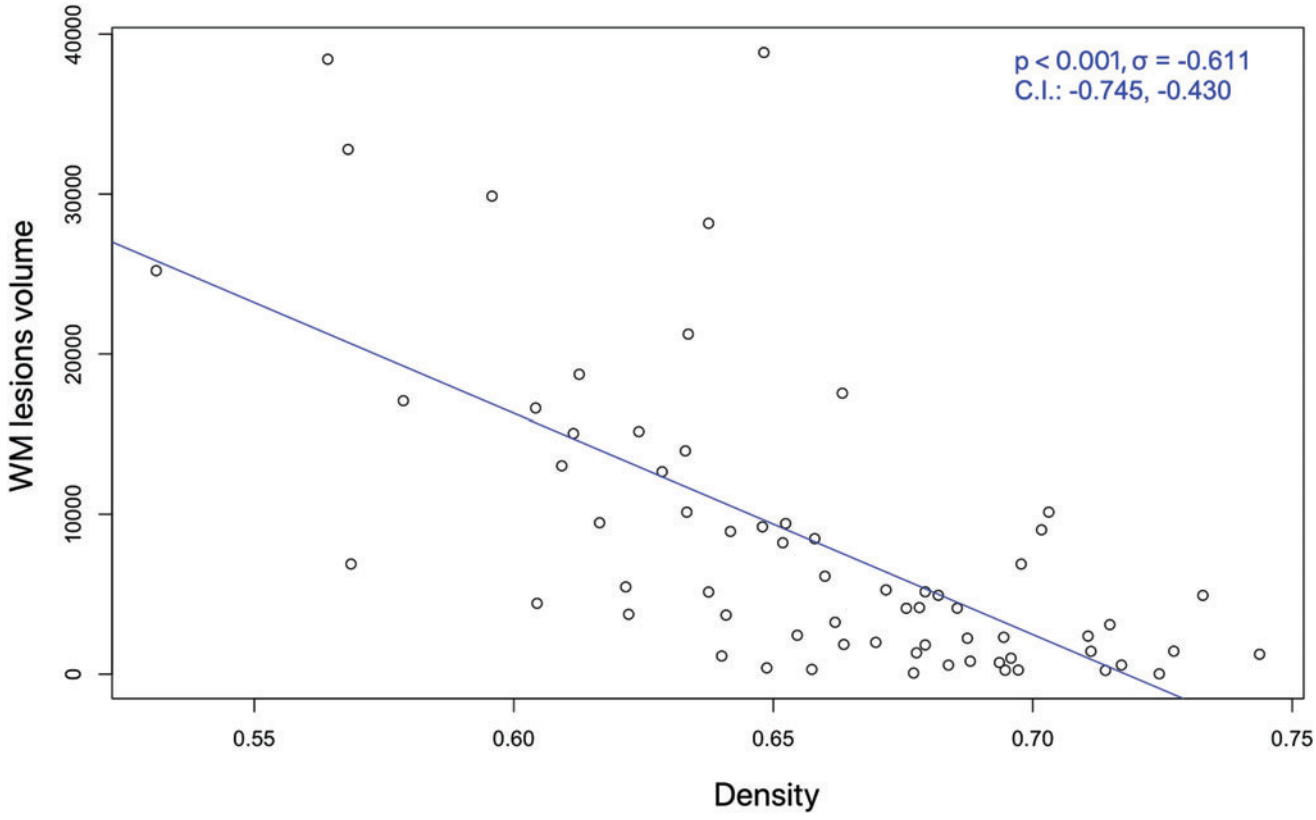

FIG. 2. Correlation between the white matter lesion volume (in mm^3) and the density of the connectomes of all MS patients involved in our study. CI, confidence interval; WM, white matter. Color images are available online.

Table 2. Comparison of Network Metrics Computed Using Different Microstructural Weightings Between Multiple Sclerosis Patients and Healthy Controls

	Network metrics	*Healthy controls*	*MS patients*	*Adjusted* p *value metrics*	*Adjusted* p *value model*
FA	Efficiency	0.410 ± 0.014	0.394 ± 0.021	0.639	1.000
	Modularity	0.065 ± 0.010	0.078 ± 0.020	0.477	0.812
	Clustering coefficient	0.382 ± 0.015	0.367 ± 0.020	0.639	1.000
	Mean strength	27.300 ± 1.400	25.500 ± 2.380	0.639	1.000
-ln(MD)	Efficiency	6.030 ± 0.087	5.900 ± 0.179	**0.020**	0.075
	Modularity	0.080 ± 0.015	0.097 ± 0.027	0.606	1.000
	Clustering coefficient	5.810 ± 0.100	5.69 ± 0.160	0.218	0.812
	Mean strength	412.000 ± 13.900	393.000 ± 28.100	**0.020**	0.062
-ln(RD)	Efficiency	6.320 ± 0.097	6.180 ± 0.196	**0.049**	0.124
	Modularity	0.078 ± 0.015	0.095 ± 0.027	0.489	1.000
	Clustering coefficient	6.080 ± 0.110	5.950 ± 0.176	0.203	0.812
	Mean strength	432.000 ± 14.800	411.00 ± 30.000	**0.049**	0.130
ICVF	Efficiency	0.499 ± 0.023	0.472 ± 0.034	**0.017**	0.057
	Modularity	0.069 ± 0.014	0.088 ± 0.026	**0.017**	0.069
	Clustering coefficient	0.470 ± 0.023	0.444 ± 0.034	**0.017**	0.069
	Mean strength	33.500 ± 2.020	30.700 ± 3.370	**0.017**	**0.050**
-ln(ISOVF)	Efficiency	2.120 ± 0.119	2.090 ± 0.131	1.000	1.000
	Modularity	0.116 ± 0.014	0.131 ± 0.025	1.000	1.000
	Clustering coefficient	1.980 ± 0.113	1.950 ± 0.119	1.000	1.000
	Mean strength	141.000 ± 9.060	135.000 ± 12.500	1.000	1.000
INTRA	Efficiency	0.486 ± 0.024	0.456 ± 0.038	**0.028**	0.077
	Modularity	0.069 ± 0.014	0.087 ± 0.025	**0.030**	0.214
	Clustering coefficient	0.456 ± 0.024	0.426 ± 0.038	**0.028**	0.077
	Mean strength	32.500 ± 2.080	29.600 ± 3.600	**0.028**	0.077
-ln(EXTRAMD)	Efficiency	5.660 ± 0.082	5.550 ± 0.161	0.174	0.261
	Modularity	0.080 ± 0.015	0.098 ± 0.027	0.794	1.000
	Clustering coefficient	5.450 ± 0.094	5.360 ± 0.143	0.794	1.000
	Mean strength	387.000 ± 13.000	369.000 ± 26.000	0.174	0.261
-ln(EXTRATRANS)	Efficiency	6.020 ± 0.101	5.870 ± 0.193	**0.023**	0.077
	Modularity	0.079 ± 0.015	0.096 ± 0.027	0.514	1.000
	Clustering coefficient	5.780 ± 0.111	5.650 ± 0.175	0.090	0.261
	Mean strength	411.000 ± 14.600	390.000 ± 28.800	**0.023**	0.070
NOS	Efficiency	2109 ± 83.500	2120 ± 104.000	0.494	/
	Modularity	0.360 ± 0.025	0.382 ± 0.039	0.867	/
	Clustering coefficient	197 ± 7.880	203 ± 9.630	0.243	/
	Mean strength	43,658 ± 1346	43,094 ± 1920	0.867	/

Results of group comparison performed with robust linear model accounting for gender, age, and density as covariates. To account for multiple comparison, we applied Holm *post hoc* correction (1) for each network metrics of each microstructural map (adjusted *p* value metrics) and (ii) for each network metrics extracted from all the microstructural maps of each diffusion-based model (adjusted *p* value model). The statistically significant results are highlighted in bold.

EXTRAMD, extraneurite mean diffusivity; EXTRATRANS, extraneurite transverse diffusivity; FA, fractional anisotropy; ICVF, intraneurite volume fraction; INTRA, neurite volume fraction; ISOVF, isotropic volume fraction; MD, mean diffusivity; MS, multiple sclerosis; NOS, number of streamlines; RD, radial diffusivity.

$R^2 = 0.535$ and adjusted $R^2 = 0.526$, respectively). Although age seemed to drive the differences, modularity also contributed significantly ($p = 0.016$ and $p = 0.028$, respectively) as given in Table 3 (we refer to Supplementary Tables S2 and S3 for more details regarding the statistical analysis).

However, we found that network metrics computed by weighting the connectomes with DTI-FA, DTI-MD, DTI-RD, NODDI-ICVF, SMT-EXTRAMD, and SMT-EXTRATRANS were associated with sNfL (adjusted $R^2 = 0.597$; adjusted $R^2 = 0.609$; adjusted $R^2 = 0.600$, adjusted $R^2 = 0.598$, adjusted $R^2 = 0.611$, adjusted $R^2 = 0.603$, respectively). Again, modularity contributed significantly, despite age and gender seem to drive the significance, as given in Table 4 ($p = 0.025$, $p = 0.033$, $p = 0.016$, $p = 0.022$, $p = 0.013$, and $p = 0.049$, respectively).

Discussion

Our tractometry study compared the sensitivity of network analysis performed using different connectomes, weighted with these advanced models, to identify differences in structural network properties in MS patients versus HCs. In addition, our study provided a clinical and biological validation of the results by assessing the relationship between (1) network measure weighted for different microstructural parameters and (2) patient's disability and (3) sNfL levels, which are a measure of neuroaxonal damage.

Previous connectomic studies in MS patients used essentially NOS or FA to weight the computed connectomes (Charalambous et al., 2019; Kamagata et al., 2019; Kocevar et al., 2016; Li et al., 2013; Llufriu et al., 2017; Pagani

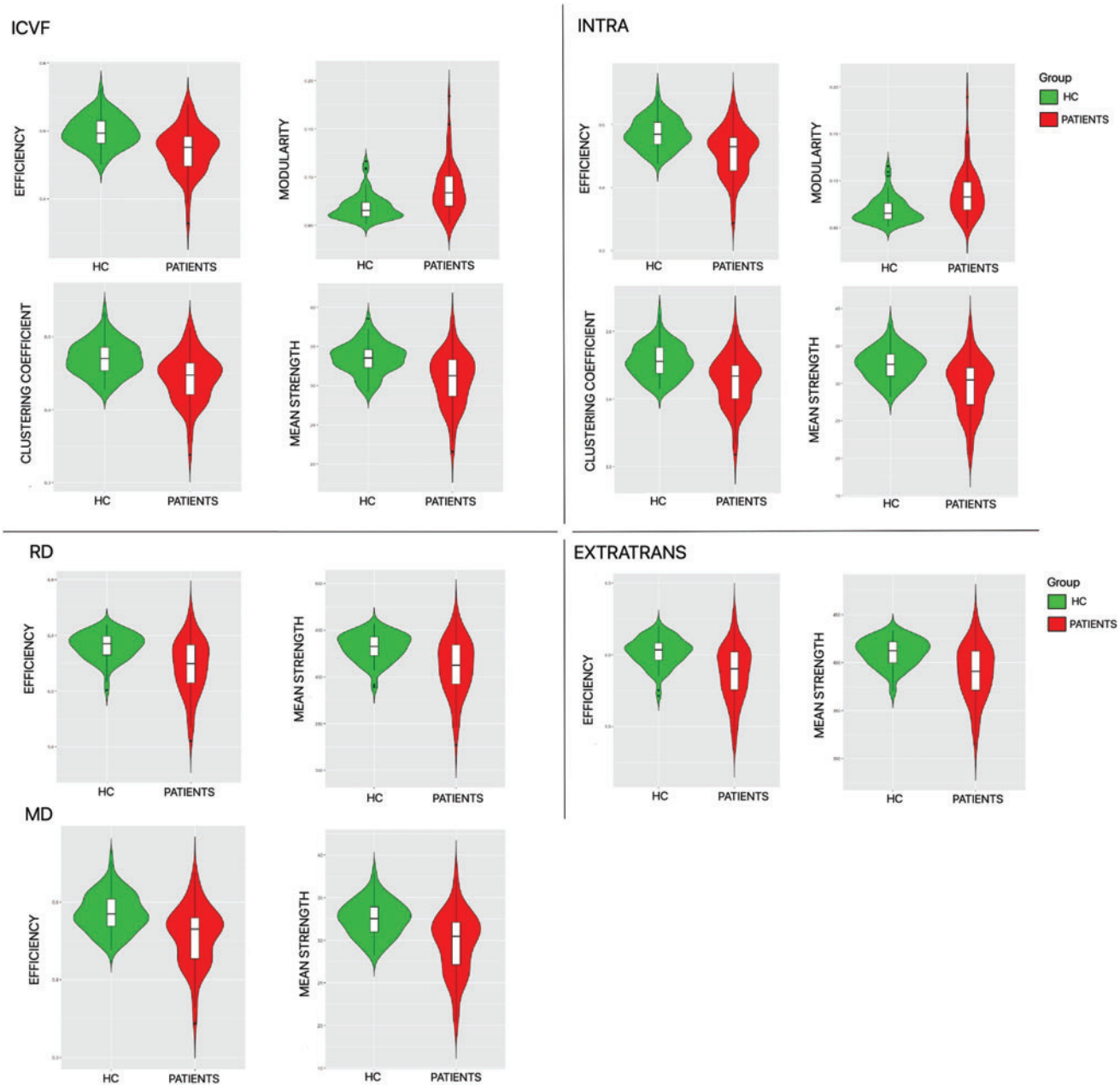

FIG. 3. Violin plots of the metrics showing statistically significant differences between HCs (in green) and multiple sclerosis patients (in red). In the upper part of the violin plots, we show the efficiency, modularity, clustering coefficient, and mean strength resulting from the connectomes weighted using ICVF and INTRA. In the bottom part, we show efficiency and mean strength resulting from the connectomes weighted using RD, EXTRATRANS, and MD. EXTRATRANS, extraneurite transverse diffusivity; HC, healthy controls; ICVF, intraneurite volume fraction; INTRA, neurite volume fraction; MD, mean diffusivity; RD, radial diffusivity. Color images are available online.

et al., 2020; Pardini et al., 2015; Shu et al., 2011, 2016), which were then used to extract network-based metrics in MS patients and HCs. These studies showed an overall decrease in patient network performances especially regarding a decrease in efficiency and an increase in network segregation.

Although these studies have proven to be sensitive to MS pathology, they lack yet specificity to the structural substrate of network alterations. Weighting the connectomes for measures derived from microstructural models applied to multi-shell diffusion data allows to achieve higher specificity to alterations occurring within specific compartments of the brain tissue (Lakhani et al., 2020).

Since MS is a complex neurological disease, which is characterized by inflammatory demyelination and axonal loss, and also by remyelination and network remodeling (Cunniffe and Coles, 2019), the information derived from network measures obtained using microstructural maps may be more sensitive and specific than the approaches based on NOS. Newly developed advanced multicompartment

Table 3. Correlation Between Network Metrics Weighted for Intraneurite Volume Fraction/Neurite Volume Fraction, and Expanded Disability Status Scale

		Estimate	*SE*	*t value*	*Pr(>|t|)*
ICVF	(Intercept)	−23.745	22.859	−1.039	0.303
Multiple R^2: 0.592; Adjusted R^2: 0.535	Density	31.724	34.456	0.921	0.361
	Efficiency	−7.735	69.011	−0.112	0.911
	Modularity	33.539	13.553	2.475	**0.016**
	Clustering coefficient	52.857	49.289	1.072	0.288
	Mean strength	−0.673	1.121	−0.600	0.551
	Gender	0.151	0.351	0.430	0.668
	Age	0.069	0.014	5.034	**<0.001**
	Disease duration	0.008	0.010	0.744	0.460
INTRA	(Intercept)	−23.546	23.784	−0.990	0.326
Multiple R^2: 0.584; Adjusted R^2: 0.526	Density	33.357	35.799	0.932	0.355
	Efficiency	3.083	76.846	0.040	0.968
	Modularity	28.678	12.690	2.260	**0.028**
	Clustering coefficient	48.160	52.987	0.909	0.367
	Mean strength	−0.798	1.187	−0.672	0.504
	Gender	0.070	0.349	0.201	0.841
	Age	0.072	0.014	5.196	**<0.001**
	Disease duration	0.007	0.010	0.677	0.501

The statistically significant results are highlighted in bold.

Robust linear models to identify the contribution of each network metrics in explaining the EDSS. Age, gender, and disease duration are included as covariates. For compactness, only the maps that show significant results are presented. In the upper part we have the model corresponding to ICVF, whereas in the bottom we have the model corresponding to INTRA. Both models explain ∼53% of our data. In the two models, in addition to age that describes most of EDSS, modularity also seems to contribute to explaining the worsening of the disease, highlighting that EDSS is related to the segregation of the network.

SE, standard error.

diffusion MRI models are in fact able to isolate the contribution of the signal deriving from the different tissue compartments, thus having the potential to detect specific tissue subtypes and associated injuries with increased pathologic specificity (Lakhani et al., 2020).

When assessing the pathological sensitivity of our network-based analysis derived from tractometry, we have found that the most sensitive microstructural measures were related to the intracellular compartment, that is, intra-axonal compartment since we focused on WM connections. Specifically, when the connectomes were weighted for both NODDI-ICVF and SMT-INTRA, we measured a significant decrease in global efficiency, clustering coefficient, and mean strength as well as a significant increase in modularity in MS patients compared with HCs. This indicates an increased network segregation, a decrease in the number of connections, and, in turn, a loss in network efficiency in MS patients, confirming and extending what was observed in Welton et al. (2020), where a normalized NOS measure was applied.

Adding to previous knowledge, our results also show a direct relationship between the observed reduction in the edge values weighted with NODDI-ICVF and SMT-INTRA and axonal damage, since these two maps describe the anisotropic signal of the intra-axonal compartment. Furthermore, it is probable that these results are also related to the demyelination that occurred in those axons, since NODDI-ICVF has been also shown to strongly correlate with the myelin fraction of a spinal cord tissue, in a recent postmortem MRI and histology study (Grussu et al., 2017). As a consequence, the reduction in efficiency, clustering coefficient, and connection strength that we measured in MS patients—together with the observed increase in modularity (and hence segregation)—may be representative of both axonal damage and demyelination in the tracts of interest. In contrast, measures of demyelination and of increased diffusivity obtained with DTI showed less sensitivity to MS pathology, whereas NOS measures appeared to be relatively insensitive.

Similarly, when we assessed the relationship between the network-based measures derived from microstructural maps and patient's disability, only the modularity measured in connectomes weighted with NODDI-ICVF and SMT-INTRA maps shows a significant relationship with patient disability, suggesting that the network segregation caused by axon myelin damage led to a disruption in network properties that is associated with the overall patient disability.

We acknowledge that EDSS is a crude measure of clinical disability and EDSS scores >5 are mainly driven by walking abilities, as well as by spinal cord damage. However, it is important to note that it is also very often the case that individuals with high disability scores and long disease duration have also an important lesion load in the brain that seem to be confirmed by our analyses. To disentangle better these two aspects, in future studies more data should be acquired for patients with EDSS ≥5 to better investigate the impact of the spinal cord damage.

Counterintuitively, when we assessed the relationship between network-based measures derived from microstructural maps and neuroaxonal damage—as measured in the serum with NfL—we found that the decrease in modularity weighted by measures of extracellular diffusivity was related to a biological increase of neuroaxonal damage. These results are quite intriguing as they may indicate that the properties of the extracellular compartment, which is essentially constituted by the extracellular matrix, interstitial fluids, and glia cells, influence the network aggregation in a way

Table 4. Correlation Between Network Metrics Weighted for Different Microstructural Measures and Serum Neurofilament Light Polypeptide

		Estimate	*SE*	*t value*	*Pr(>|t|)*
FA	(Intercept)	2.488	12.122	0.205	0.838
Multiple R^2: 0.649; Adjusted R^2: 0.597	Density	−5.219	18.413	−0.283	0.778
	Efficiency	−25.316	44.521	−0.569	0.572
	Modularity	10.774	4.663	2.310	**0.025**
	Clustering coefficient	10.402	16.795	0.619	0.539
	Mean strength	0.274	0.716	0.383	0.703
	Gender	0.212	0.091	2.339	**0.024**
	Age	0.023	0.003	6.634	**<0.001**
MD	(Intercept)	−0.017	0.937	−1.801	0.078
Multiple R^2: 0.660; Adjusted R^2: 0.609	Density	0.025	0.0138	1.800	0.078
	Efficiency	0.456	0.260	1.755	0.086
	Modularity	7.297	3.330	2.192	**0.033**
	Clustering coefficient	1.147	1.041	1.102	0.276
	Mean strength	−0.689	0.3856	−1.787	0.080
	Gender	0.255	0.096	2.658	**0.011**
	Age	0.019	0.003	5.439	**<0.001**
RD	(Intercept)	−70.348973	63.352860	−1.110	0.272
Multiple R^2: 0.652; Adjusted R^2: 0.600	Density	104.913926	98.913304	1.061	0.294
	Efficiency	17.315908	16.691008	1.037	0.305
	Modularity	8.127231	3.249140	2.501	**0.016**
	Clustering coefficient	1.020346	1.005984	1.014	0.316
	Mean strength	−0.271909	0.256680	−1.059	0.295
	Gender	0.235082	0.094214	2.495	**0.016**
	Age	0.019849	0.003594	5.522	**<0.001**
ISOVF	(Intercept)	−2.588	8.710	−0.297	0.768
Multiple R^2: 0.650; Adjusted R^2: 0.598	Density	3.139	13.664	0.230	0.819
	Efficiency	−2.507	5.519	−0.454	0.652
	Modularity	8.077	3.415	2.365	**0.022**
	Clustering coefficient	3.588	3.125	1.148	0.257
	Mean strength	−0.011	0.094	−0.114	0.910
	Gender	0.221	0.089	2.481	**0.017**
	Age	0.020	0.003	5.710	**<0.001**
EXTRAMD	(Intercept)	−0.018	0.018	−1.639	0.108
Multiple R^2: 0.66; Adjusted R^2: 0.611	Density	0.025	0.016	1.558	0.126
	Efficiency	0.509	0.318	1.599	0.116
	Modularity	8.502	3.297	2.579	**0.013**
	Clustering Coefficient	1.455	1.128	1.290	0.203
	Mean strength	−0.749	0.474	−1.580	0.121
	Gender	0.270	0.094	2.880	**0.006**
	Age	0.018	0.004	4.857	**<0.001**
EXTRATRANS	(Intercept)	−64.478	33.700	−1.913	0.062
Multiple R^2: 0.655; Adjusted R^2: 0.603	Density	102.322	54.520	1.877	0.069
	Efficiency	16.863	9.344	1.805	0.077
	Modularity	6.648	3.295	2.018	**0.049**
	Clustering coefficient	0.840	1.047	0.803	0.426
	Mean strength	−0.273	0.147	−1.861	0.069
	Gender	0.248	0.095	2.606	**0.012**
	Age	0.020	0.003	5.670	**<0.001**

The statistically significant results are highlighted in bold.

Robust linear models to identify the correlation between the changes in the structural connectivity of MS patients through the global network metrics and the increase of sNfL. Age and gender are included as covariates. For compactness, only the maps that show significant results are presented. Both models explain ~60% of our data. In the six models, in addition to age, which explain most of sNfL increase, gender and modularity also seem to contribute to explaining the increase of NfL blood concentration, highlighting that the network segregation is related to increased inflammation and axonal damage.

sNfL, serum neurofilament light polypeptide.

that is, in part, proportional to neuroaxonal damage (Van Horssen et al., 2007). Network metrics obtained with connectomes weighted for NOS did not show any correlation with both patients' EDSS and sNfL.

It is important to remark that the lesions of MS patients are characterized by voxels containing different types of tissue, which makes tissue segmentation critical for those voxels. For this reason, we have decided to use the multishell multitissue constrained spherical deconvolution algorithm, which is able to take into account partial volume effects and allows to estimate the fiber orientation distribution in multiple tissues, even within the same voxel. The obtained estimation

of the FODs, in combination with the iFOD2 tracking algorithm (Tournier et al., 2010) constrained to a deterministic-like behavior, guarantees the reconstruction of the streamlines even in lesion voxels (Lipp et al., 2020). Thus, even in the areas affected by lesions, the connectivity is not completely disrupted.

Nevertheless, in very damaged lesions, there may be no residual anisotropic tissue, leading, therefore, to the estimation of few connections (Van Wijk et al., 2010). This causes a decrease in connection density of the connectomes that is negatively correlated with the volume of the WM lesions as shown in Figure 2, and very damaged lesions may also significantly impact the microstructural properties of the entire tract they affect. In light of this, and to grant a fair comparison between connectomes of the two groups of subjects (Schiavi et al., 2020b), we used the connection density as a confounding factor in our statistical analyses. Nevertheless, it has to be acknowledged that the impact of very destructive lesions will be more evident on NOS-weighted connectomes than in connectomes weighted by other microstructural measures.

Limitations of our study are related to the small number of enrolled patients, which did not allow us to perform a proper comparison of the sensitivity and biological correlation of microstructure-weighted network metrics between progressive and relapsing-remitting patients. We have, however, computed the results of the group comparison between relapsing remitting MS patients and HCs (Supplementary Table S1), which showed very similar results to those obtained in the whole cohort. In a follow-up study, we will expand the cohort by including more progressive patients. Another limitation of this study is related to the fact that sNfL was assessed within 3 months from the MRI, hence we cannot exclude that disease-related or unrelated factors may have affected sNfL values. Furthermore, in this study we have focused on the relationship between network metrics derived from microstructural-weighted connectomes and disability or biological biomarkers of disease impact (i.e., sNfL).

Future studies will also attempt at assessing the value of weighting the connectomes with myelin-specific measures such as myelin water fraction and quantitative magnetization transfer (Granziera et al., 2020; Koenig et al., 1990; Mackay et al., 1994; Mossahebi et al., 2014, 2015). Finally, another interesting point for the future could be to evaluate the sensitivity to the pathology by weighting the connectomes using the newly proposed anatomically constrained microstructure-informed tractography (Daducci et al., 2014; Schiavi et al., 2020a).

Conclusion

In conclusion, we have shown that network-derived metrics in MS patients are most sensitive to MS pathology and most related to clinical disability when connectomes are weighted for intracellular/intra-axonal microstructural metrics, whereas connectomes weighted for extracellular diffusivity permit to assess network metrics that are most related to biological measures of neuroaxonal damage.

Acknowledgments

We thank Mrs. Marguerite Limberg for her precious contribution in enrolling study participants. And we thank all the patients and HCs for their contribution.

Authors' Contributions

S.B., Si.S., A.D., and C.G. contributed to conception and design of the study; S.B., Si.S., Sa.S., P.J.L., M.B., and M.W. analyzed data; P.J.L., M.B., and M.W. acquired data; S.B., Si.S., A.D., and C.G. drafted a significant portion of the article and figures; S.B., Si.S., Sa.S., P.J.L., M.B., M.W., L.K., J.K., A.D., and C.G. revised the final article; funding was taken care of L.K., J.K., A.D., and C.G.

Author Disclosure Statement

All authors have nothing to disclose for the purpose of this study.

Funding Information

S.B., Si.S., Sa.S., P.J.L., M.B., L.K., J.K., and A.D declare no funding was received. M.W. is paid by the Swiss National Science Foundation (SNSF) grant PP00P3_176984 and he has also received research funding by Biogen for developing spinal cord MRI. C.G. is funded by the Swiss National Science Foundation (SNSF) grant PP00P3_176984, the Stiftung zur Förderung der gastroenterologischen und allgemeinen klinischen Forschung, EUROSTAR E!113682 HORIZON2020.

Supplementary Material

Supplementary Table S1
Supplementary Table S2
Supplementary Table S3

References

Aickin M, Gensler H. 1996. Adjusting for multiple testing when reporting research results: the Bonferroni vs Holm methods. Am J Public Health 86:726–728.

Alexander DC, Dyrby TB, Nilsson M, et al. 2019. Imaging brain microstructure with diffusion MRI: practicality and applications. NMR Biomed 32:e3841.

Bells S, Cercignani M, Deoni S, et al. 2011. ''Tractometry''—comprehensive multi-modal quantitative assessment of white matter along specific tracts. Proc Int Soc Magn Reson Med 19:678.

Buchanan CR, Bastin ME, Ritchie SJ, et al. 2020. The effect of network thresholding and weighting on structural brain networks in the UK Biobank. Neuroimage 211:116443.

Charalambous T, Tur C, Prados F, et al. 2019. Structural network disruption markers explain disability in multiple sclerosis. J Neurol Neurosurg Psychiatry 90:219–226.

Cunniffe N, Coles A. 2019. Promoting remyelination in multiple sclerosis. J Neurol 268:30–44.

Daducci A, Canales-Rodríguez EJ, Zhang H, et al. 2015. Accelerated microstructure imaging via convex optimization (AMICO) from diffusion MRI data. Neuroimage 105: 32–44.

Daducci A, Dal Palù A, Lemkaddem A, et al. 2014. COMMIT: convex optimization modeling for microstructure informed tractography. IEEE Trans Med Imaging 34:246–257.

Descoteaux M. 2008. *High Angular Resolution Diffusion MRI: from Local Estimation to Segmentation and Tractography*. Université Nice Sophia Antipolis.

Desikan RS, Ségonne F, Fischl B, et al. 2006. An automated labeling system for subdividing the human cerebral cortex on MRI scans into gyral based regions of interest. Neuroimage 31:968–980.

Devan SP, Jiang X, Bagnato F, et al. 2020. Optimization and numerical evaluation of multi-compartment diffusion MRI using the spherical mean technique for practical multiple sclerosis imaging. Magn Reson Imaging 74:56–63.

Disanto G, Barro C, Benkert P, et al. 2017. Serum Neurofilament light: a biomarker of neuronal damage in multiple sclerosis. Ann Neurol 81:857–870.

Fleischer V, Radetz A, Ciolac D, et al. 2019. Graph theoretical framework of brain networks in multiple sclerosis: a review of concepts. Neuroscience 403:35–53.

Gamboa OL, Tagliazucchi E, Von Wegner F, et al. 2014. Working memory performance of early MS patients correlates inversely with modularity increases in resting state functional connectivity networks. Neuroimage 94:385–395.

Gibbs E, Liu C. 2015. Feasibility of imaging tissue electrical conductivity by switching field gradients with MRI. Tomography 1:125–135.

Granziera C, Wuerfel J, Barkhof F, et al. 2020. Quantitative magnetic resonance imaging towards clinical application in multiple sclerosis. Brain 144:1296–1311.

Griffa A, Baumann PS, Thiran JP, et al. 2013. Structural connectomics in brain diseases. Neuroimage 80:515–526.

Grussu F, Schneider T, Tur C, et al. 2017. Neurite dispersion: a new marker of multiple sclerosis spinal cord pathology? Ann Clin Transl Neurol 4:663–679.

He Y, Dagher A, Chen Z, et al. 2009. Impaired small-world efficiency in structural cortical networks in multiple sclerosis associated with white matter lesion load. Brain 132:3366–3379.

Horsfield MA. 1999. Mapping eddy current induced fields for the correction of diffusion-weighted echo planar images. Magn Reson Imaging 17:1335–1345.

Jenkinson M, Bannister P, Brady M, et al. 2002. Improved optimization for the robust and accurate linear registration and motion correction of brain images. Neuroimage 17:825–841.

Jones DK, Knösche TR, Turner R. 2013. White matter integrity, fiber count, and other fallacies: the do's and don'ts of diffusion MRI. Neuroimage 73:239–254.

Kaden E, Kelm ND, Carson RP, et al. 2016. Multi-compartment microscopic diffusion imaging. Neuroimage 139:346–359.

Kaden E, Kruggel F, Alexander DC. 2015. Quantitative mapping of the per-axon diffusion coefficients in brain white matter. Magn Reson Med 75:1752–1763.

Kamagata K, Zalesky A, Yokoyama K, et al. 2019. MR g-ratio-weighted connectome analysis in patients with multiple sclerosis. Sci Rep 9:13522.

Khalil M, Teunissen CE, Otto M, et al. 2018. Neurofilaments as biomarkers in neurological disorders. Nat Rev Neurol 14: 577–589.

Kocevar G, Stamile C, Hannoun S, et al. 2016. Graph theory-based brain connectivity for automatic classification of multiple sclerosis clinical courses. Front Neurosci 10:478.

Koenig SH, Brown III RD, Spiller M, et al. 1990. Relaxometry of brain: why white matter appears bright in MRI. Magn Reson Med 14:482–495.

Koller M, Stahel WA. 2011. Sharpening Wald-type inference in robust regression for small samples. Comput Stat Data Analysis 55:2504–2515.

Kurtzke JF. 2009. Rating neurological impairment in multiple sclerosis: an expanded disability status scale. Neurology 1983.

Lakhani DA, Schilling KG, Xu J, et al. 2020. Advanced multi-compartment diffusion MRI models and their application in multiple sclerosis. Am J Neuroradiol 41:751–757.

La Rosa F, Abdulkadir A, Fartaria MJ, et al. 2020. Multiple sclerosis cortical and WM lesion segmentation at 3T MRI: a deep learning method based on FLAIR and MP2RAGE. Neuroimage Clin 27:102335.

Le Bihan D, Mangin J-F, Poupon C, et al. 2001. Diffusion tensor imaging: concepts and applications. J Magn Reson Imaging 13:534–546.

Li Y, Jewells V, Kim M, et al. 2013. Diffusion tensor imaging based network analysis detects alterations of neuroconnectivity in patients with clinically early relapsing-remitting multiple sclerosis. Hum Brain Mapp 34:3376–3391.

Lipp I, Parker GD, Tallantyre EC, et al. 2020. Tractography in the presence of multiple sclerosis lesions. NeuroImage 209: 116471.

Llufriu S, Martinez-Heras E, Solana E, et al. 2017. Structural networks involved in attention and executive functions in multiple sclerosis. Neuroimage Clin 13:288–296.

Mackay A, Whittall K, Adler J, et al. 1994. *In vivo* visualization of myelin water in brain by magnetic resonance. Magn Reson Med 31:673–677.

Mossahebi P, Alexander AL, Field AS, et al. 2015. Removal of cerebrospinal fluid partial volume effects in quantitative magnetization transfer imaging using a three-pool model with nonexchanging water component. Magn Reson Med 74:1317–1326.

Mossahebi P, Yarnykh VL, Samsonov A. 2014. Analysis and correction of biases in cross-relaxation MRI due to biexponential longitudinal relaxation. Magn Reson Med 71:830–838.

Nigro S, Passamonti L, Riccelli R, et al. 2015. Structural connectomic alterations in the limbic system of multiple sclerosis patients with major depression. Mult Scler 21:1003–1012.

O'Donnell LJ, Westin C-F. 2011. An introduction to diffusion tensor image analysis. Neurosurg Clin N Am 22:185–196, viii.

Ozturk A, Smith SA, Gordon-Lipkin EM, et al. 2010. MRI of the corpus callosum in multiple sclerosis: association with disability. Mult Scler 16:166–177.

Pagani E, Rocca MA, De Meo E, et al. 2020. Structural connectivity in multiple sclerosis and modeling of disconnection. Mult Scler J 26:220–232.

Pardini M, Yaldizli Ö, Sethi V, et al. 2015. Motor network efficiency and disability in multiple sclerosis. Neurology 85: 1115–1122.

Richiardi J, Gschwind M, Simioni S, et al. 2012. Classifying minimally disabled multiple sclerosis patients from resting state functional connectivity. Neuroimage 62:2021–2033.

Rocca MA, Valsasina P, Absinta M, et al. 2010. Default-mode network dysfunction and cognitive impairment in progressive MS. Neurology 74:1252–1259.

Rocca MA, Valsasina P, Meani A, et al. 2016. Impaired functional integration in multiple sclerosis: a graph theory study. Brain Struct Funct 221:115–131.

Rolak LA. 2003. Multiple sclerosis: it's not the disease you thought it was. Clin Med Res 1:57–60.

Sarwar T, Ramamohanarao K, Zalesky A. 2019. Mapping connectomes with diffusion MRI: deterministic or probabilistic tractography? Magn Reson in Med 81:1368–1384.

Schiavi S, Ocampo-Pineda M, Barakovic M, et al. 2020a. A new method for accurate in vivo mapping of human brain connections using microstructural and anatomical information. Sci Adv 6:eaba8245.

Schiavi S, Petracca M, Battocchio M, et al. 2020b. Sensory-motor network topology in multiple sclerosis: structural connectivity analysis accounting for intrinsic density discrepancy. Hum Brain Mapp 41:2951–2963.

Shu N, Duan Y, Xia M, et al. 2016. Disrupted topological organization of structural and functional brain connectomes in clinically isolated syndrome and multiple sclerosis. Sci Rep 6:29383.

Shu N, Liu Y, Li K, et al. 2011. Diffusion tensor tractography reveals disrupted topological efficiency in white matter structural networks in multiple sclerosis. Cerebral Cortex 21:2565–2577.

Smith R, Raffelt D, Tournier J-D, et al. 2020. Quantitative streamlines tractography: methods and inter-subject normalisation.

Smith RE, Tournier J-D, Calamante F, et al. 2012. Anatomically-constrained tractography: improved diffusion MRI streamlines tractography through effective use of anatomical information. Neuroimage 62:1924–1938.

Sotiropoulos SN, Zalesky A. 2019. Building connectomes using diffusion MRI: why, how and but. NMR Biomed 32:e3752.

Tewarie P, Hillebrand A, Schoonheim MM, et al. 2014. Functional brain network analysis using minimum spanning trees in Multiple Sclerosis: An MEG source-space study. Neuroimage 88:308–318.

Thompson AJ, Banwell BL, Barkhof F, et al. 2018. Diagnosis of multiple sclerosis: 2017 revisions of the McDonald criteria. Lancet Neurol 17:162–173.

Tournier JD, Calamante F, Connelly A. 2010. Improved probabilistic streamlines tractography by 2nd order integration over fibre orientation distributions. Ismrm.

Tournier J-DD, Smith R, Raffelt D, et al. 2019. MRtrix3: a fast, flexible and open software framework for medical image processing and visualisation. Neuroimage 202:116137.

Van Horssen J, Dijkstra CD, De Vries HE. 2007. The extracellular matrix in multiple sclerosis pathology. J Neurochem 103:1293–1301.

Van Wijk BCMM, Stam CJ, Daffertshofer A. 2010. Comparing brain networks of different size and connectivity density using graph theory. PLoS One 5:e13701.

Welton T, Constantinescu CS, Auer DP, et al. 2020. Graph theoretic analysis of brain connectomics in multiple sclerosis: reliability and relationship with cognition. Brain Connect 10:95–104.

Yamada H, Abe O, Shizukuishi T, et al. 2014. Efficacy of distortion correction on diffusion imaging: comparison of FSL eddy and eddy-correct using 30 and 60 directions diffusion encoding. PLoS One 9:e112411.

Yeh CH, Jones DK, Liang X, et al. 2020. Mapping structural connectivity using diffusion MRI: challenges and Opportunities. J Magn Reson Imaging 53:1666–1682.

Zalesky A, Fornito A, Bullmore ET. 2010. Network-based statistic: identifying differences in brain networks. Neuroimage 53:1197–1207.

Zhang H, Schneider T, Wheeler-Kingshott CA, et al. 2012. NODDI: practical *in vivo* neurite orientation dispersion and density imaging of the human brain. Neuroimage 61:1000–1016.

Address correspondence to:
Cristina Granziera
Translational Imaging in Neurology (ThINk)
Department of Biomedical Engineering
University Hospital Basel and University of Basel
Gewerbestrasse 16
4123 Allschwil, BL
Switzerland

E-mails: cristina.granziera@usb.ch;
cristina.granziera@unibas.ch